Silencing the Flavonoid Pathway in *Medicago truncatula* Inhibits Root Nodule Formation and Prevents Auxin Transport Regulation by Rhizobia [W]

Anton P. Wasson, Flavia I. Pellerone, and Ulrike Mathesius[1]

School of Biochemistry and Molecular Biology, Australian Research Council Centre of Excellence for Integrative Legume Research, Australian National University, Canberra ACT 0200, Australia

Legumes form symbioses with rhizobia, which initiate the development of a new plant organ, the nodule. Flavonoids have long been hypothesized to regulate nodule development through their action as auxin transport inhibitors, but genetic proof has been missing. To test this hypothesis, we used RNA interference to silence chalcone synthase (CHS), the enzyme that catalyzes the first committed step of the flavonoid pathway, in *Medicago truncatula*. *Agrobacterium rhizogenes* transformation was used to create hairy roots that showed strongly reduced CHS transcript levels and reduced levels of flavonoids in silenced roots. Flavonoid-deficient roots were unable to initiate nodules, even though normal root hair curling was observed. Nodule formation and flavonoid accumulation could be rescued by supplementation of plants with the precursor flavonoids naringenin and liquiritigenin. The flavonoid-deficient roots showed increased auxin transport compared with control roots. Inoculation with rhizobia reduced auxin transport in control roots after 24 h, similar to the action of the auxin transport inhibitor *N*-(1-naphthyl)phthalamic acid (NPA). Rhizobia were unable to reduce auxin transport in flavonoid-deficient roots, even though NPA inhibited auxin transport. Our results present genetic evidence that root flavonoids are necessary for nodule initiation in *M. truncatula* and suggest that they act as auxin transport regulators.

INTRODUCTION

Flavonoids are a diverse class of metabolites with a colorful array of functions in plants, ranging from plant pigments to antioxidants and auxin transport inhibitors (Winkel-Shirley, 2001). Many plant species also use flavonoids as signals and defense compounds in their interactions with beneficial and pathogenic microbes. Legume roots exude specific flavonoids into the surrounding soil, which act as chemotactic signals for symbiotic nitrogen-fixing bacteria called rhizobia. The exuded flavonoids also activate the expression of *nod* genes in rhizobia (Redmond et al., 1986; Djordjevic et al., 1987; Peters and Long, 1988). *nod* genes are responsible for the synthesis of Nod factors, the bacterial signals that are necessary for the initiation of a new plant organ, the nodule (Dénarié and Debellé, 1996). Nod factors are perceived by a receptor in the legume host (Madsen et al., 2003; Radutoiu et al., 2003; Ane et al., 2004) and trigger a sequence of events, including curling of root hairs around the invading rhizobia, the entry of the rhizobia into the plant through infection threads, and the development of the nodule. Nodule formation is continually regulated by both partners and involves mechanisms controlling nodule position and numbers (Nishimura et al., 2002; Penmetsa et al., 2003; Searle et al., 2003).

Even though the early infection events in the root hairs have been studied in detail using a number of nodulation mutants defective in Nod factor perception and early signal transduction, it is not well understood how rhizobia induce the nodule primordium in the root. In indeterminate legumes, nodule development starts with the initiation of cell divisions in the inner root cortex and pericycle. It has been hypothesized that flavonoids are involved in the initiation of the nodule through their action on the plant hormone auxin and could thus play a developmental role in addition to their action as *nod* gene regulators (Hirsch, 1992).

Several lines of evidence suggest a role for auxin in nodule organogenesis. First, synthetic auxin transport inhibitors can induce the development of pseudonodules on plant roots (Allen et al., 1953; Hirsch et al., 1989). Accordingly, the application of Nod factors reduces the auxin transport capacity in roots of vetch (*Vicia sativa*) (Boot et al., 1999) and white clover (*Trifolium repens*) (Mathesius et al., 1998a). Secondly, auxin localization is correlated with the site of cortical cell division. Auxin was localized in *Lotus japonicus* and white clover roots during nodulation, using an auxin responsive promoter (*GH3*) fused to a β-glucuronidase (GUS) or green fluorescent protein (GFP) reporter gene (Mathesius et al., 1998a; Pacios-Bras et al., 2003). Reporter gene expression was located in the first dividing cells of the inner or outer cortex, from where nodules are initiated in white clover and *L. japonicus*, respectively. In addition, expression of the gene encoding the auxin import carrier AUX1 in developing nodule primordia of *Medicago truncatula* suggested that

regulation of auxin transport is necessary for nodule induction (de Billy et al., 2001).

How do rhizobia interfere with auxin transport in the plant? Auxin is largely synthesized in the shoot and transported to the root by at least two transport systems, in the phloem and by active polar transport through auxin transporters (Bennett et al., 1998; Muday and DeLong, 2001). Transporters include the auxin importer, AUX1, and a class of auxin export facilitator proteins (PIN proteins), whose asymmetric distribution on either the basal or apical side of cells controls the polarity of auxin transport (Gälweiler et al., 1998; Müller et al., 1998; Swarup et al., 2001). Most likely, PIN proteins interact with so-called multidrug resistance proteins that may modify the action of PINs (Noh et al., 2001). Auxin transport can be reduced by synthetic auxin transport inhibitors, including N-(1-naphthyl)phthalamic acid (NPA), which was shown to interfere with the intracellular cycling of the PIN proteins between the plasma membrane and endosomal vesicles in the presence of brefeldin A, an inhibitor of endosomal transport (Geldner et al., 2001). Nod factors are not similar in structure to any known auxin transport regulators, suggesting that an intermediate signaling molecule is involved in the regulation of auxin transport.

Auxin transport can be regulated by certain flavonoids, in particular the flavonols quercetin and kaempferol (Stenlid, 1976; Jacobs and Rubery, 1988). It has been hypothesized that rhizobia induce the synthesis of flavonoids in their hosts to interfere with auxin transport (Hirsch et al., 1989; Hirsch, 1992). Numerous studies have shown that rhizobia induce flavonoid synthesis in the root during nodulation (Recourt et al., 1992; Djordjevic et al., 1997; McKhann et al., 1997; Mathesius et al., 1998b). In white clover, application of the flavonoids quercetin, kaempferol, and apigenin has similar effects on the expression of GH3:GUS as NPA and Nod factors (Mathesius et al., 1998a). Despite this correlative evidence, there is no genetic proof that flavonoids are required in legumes to regulate auxin transport to facilitate nodule initiation.

A flavonoid-deficient chalcone synthase (CHS) mutant of Arabidopsis thaliana (tt4) has been identified. It shows increased auxin transport rates and is defective in auxin-regulated phenotypes, including lateral root formation and gravitropism (Brown et al., 2001; Buer and Muday, 2004; Peer et al., 2004). In legumes, no flavonoid-deficient mutants have been identified, probably because many genes of the flavonoid pathway are part of multigene families (Ryder et al., 1987; Wingender et al., 1989). To test the hypothesis that flavonoids are necessary for the regulation of auxin transport during nodule initiation, we silenced the flavonoid pathway using RNA interference (RNAi). RNAi was achieved using the binary vector pHellsgate8, from which the target sequence is expressed as an intron-spliced hairpin RNA (ihpRNA) (Wesley et al., 2001). ihpRNA was shown to be the most efficient inducer of RNAi (Smith et al., 2000). We used the model legume M. truncatula because it is easily transformable by Agrobacterium rhizogenes, forming hairy roots within a few weeks that can be successfully nodulated by its symbiont, Sinorhizobium meliloti (Boisson-Dernier et al., 2001). RNAi has recently been shown to efficiently silence the isoflavonoid pathway in soybean (Glycine max), leading to enhanced infection by the pathogen Phytophthora sojae (Subramanian et al., 2005).

We targeted the entire flavonoid pathway because it is not known which flavonoids in legumes are responsible for auxin transport inhibition nor was it the purpose of this study to identify those flavonoid(s). CHS catalyzes the first committed step of the flavonoid pathway, the synthesis of naringenin chalcone, from which the diverse flavonoid end products are derived (Stafford, 1990). We show here that silencing of CHS in M. truncatula induces flavonoid deficiency, inhibits nodulation, and disables the inhibition of auxin transport by rhizobia.

RESULTS

Silencing of the Flavonoid Pathway in *M. truncatula* Hairy Roots

A. rhizogenes transformation typically produced hairy roots emerging from the cut surface of the roots after 1 week. Untransformed adventitious roots, emerging from the hypocotyl several days after A. rhizogenes inoculation, were excised from the plantlets. RT-PCR using primers that could amplify all copies of CHS mRNA identified in The Institute for Genomic Research (TIGR) database was used to confirm gene knockdown in the CHS-silenced roots compared with control hairy roots transformed with an empty vector. We correlated CHS expression with two other phenotypes that we observed to differ between control and CHS-silenced roots: autofluorescence of the roots and the ability to nodulate (these phenotypes are further examined below).

Empty vector control and CHS-silenced hairy root plantlets were grown on agar plates and screened for autofluorescence of the roots under a fluorescence microscope. All control roots showed blue fluorescence, whereas 75% of CHS-silenced roots were devoid of blue fluorescence (Table 1). Roots were inoculated with S. meliloti, and nodule development was recorded after 2 weeks. Approximately 20% of fluorescent roots nodulated, this was similar for fluorescent control and fluorescent CHS-silenced roots, but none of the nonfluorescent CHS-silenced roots nodulated (Table 1). We then excised individual roots from control and both fluorescent and nonfluorescent CHS-silenced plantlets and tested each root for expression levels of CHS using RT-PCR (Figure 1A). All 100% (21 of 21) of the empty vector control hairy roots and 87.5% (7 of 8) of the CHS-silenced roots that remained fluorescent continued to express CHS, with similar CHS expression levels between nodulated and non-nodulated roots (data not shown). In the nonfluorescent CHS-silenced roots, only 5.3% (1 of 19) of the roots had detectable CHS expression (Table 1). Therefore, we concluded that nonfluorescent CHS-silenced roots have significantly reduced levels of CHS transcript, that fluorescence of the roots is a useful marker to screen for transformed roots, and that the cotransformation efficiency is ~75%. This cotransformation efficiency is similar to other reports of RNAi silencing in M. truncatula using A. rhizogenes (Limpens et al., 2004). In contrast with transformed hairy roots, CHS transcript levels in the leaves of the composite plants were unaltered, indicating that the RNAi effect was not systemic (Figure 1B).

To confirm that the silencing of CHS led to a reduction of flavonoid metabolites inside the root tissue, we used three assays:

Table 1. Correlation of Intracellular Fluorescence to *CHS* Expression and Nodulation

	Hairy Roots: Control Construct Transformed	Hairy Roots: CHS Silencing Construct Transformed	
		Fluorescent	Nonfluorescent
Percentage (and number) of roots fluorescing	100% (103/103)	25.2% (32/127)	74.8% (95/127)
Percentage (and number) of roots nodulating	19.4% (20/103)	18.8% (6/32)	0% (0/95)
Percentage (and number) of roots expressing CHS	100% (21/21)[a]	87.5% (7/8)[a]	5.3% (1/19)[a]

[a] For this experiment, *CHS* expression was determined in individual hairy roots of the same plants scored for fluorescence and nodulation. Representative PCR results of each of the three types of roots are shown in Figure 1A.

HPLC, thin layer chromatography (TLC), and fluorescence microscopy. For HPLC, non-nodulated roots were extracted with acetone, the flavonoids were acid-hydrolyzed to convert the glycosides to free flavonoids, and the extracted cell contents were separated and detected by their absorbance. We detected formononetin, daidzein, and medicarpin as the main flavonoid aglycones in the hairy roots of empty vector controls (Figure 2A). Levels of the identified flavonoids were reduced significantly in the extracts of CHS-silenced roots (Figure 2A). The identity of the flavonoids was established using commercially available standards run under identical conditions and comparing retention times and absorbance spectra of each standard against each of the separated peaks (Figures 2C to 2H). None of the other standards (see Methods) were detected in the root extracts. Fluorescence detection showed two major peaks at the same retention times as formononetin and medicarpin that were significantly reduced in CHS-silenced roots (see Supplemental Figure 1 online). Using TLC, we detected four fluorescent bands in the extracts of empty vector control roots. Very faint or no fluorescence was detected in extracts of CHS-silenced roots (see Supplemental Figure 2 online).

Figure 1. RT-PCR for *CHS* in Control and Silenced Hairy Roots.

(A) RT-PCR of individual roots showing examples of *CHS* expression in fluorescent (FL) empty vector control hairy root, fluorescent CHS-silenced root, and nonfluorescent (non-FL) CHS-silenced root. Actin was used as a loading control. Numbers of roots in each category showing these RT-PCR results are shown in Table 1.
(B) RT-PCR for *CHS* in roots and leaves of empty vector control (with fluorescent roots) and CHS-silenced (with nonfluorescent roots) hairy root plantlets. Approximately 10 roots or leaves were pooled for these experiments. Actin was used as a loading control.
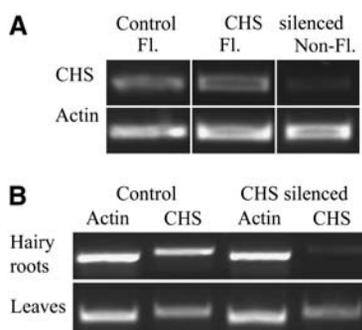
As we previously noted that blue root fluorescence was correlated with *CHS* expression levels, and because most flavonoids are fluorescent under UV light, we further examined empty vector control and CHS-silenced roots using epifluorescence microscopy. We used diphenyl boric acid-2-aminoethyl ester (DPBA), which is known to enhance the fluorescence of flavonoids in plant tissue (Neu, 1956; Sheahan and Rechnitz, 1992; Vogt et al., 1994). Control hairy roots autofluoresced bright blue under UV illumination, especially near the root tip (Figure 3A), whereas CHS-silenced hairy roots were devoid of blue intracellular autofluorescence (Figure 3B). Vibratome sections of control hairy roots showed that the blue autofluorescence was located in the cortical cells (Figure 3C). Staining with DPBA shifted the fluorescence emission of cortical and root hair fluorescence to a longer wavelength, suggesting that it was due to the presence of flavonoids (Figure 3E). Strong fluorescence was also detected in and around root hairs (Figure 3E). Sections of CHS-silenced roots lacked cortical intracellular autofluorescence (Figure 3D), and no enhanced fluorescence was observed after staining with DPBA in cortical or root hair cells (Figure 3F).

To quantify the occurrence of intracellular fluorescence, we serially sectioned 16 roots from control and CHS-silenced hairy roots. In the controls, 83% of the cortical cells of the control roots contained the blue fluorescence compared with 5% of the cortical cells of the CHS-silenced roots. While the CHS-silenced hairy roots lacked flavonoids, untransformed adventitious roots emerging from the hypocotyl contained flavonoid-based fluorescence.

CHS-Silenced Hairy Roots Are Unable to Form Nodules
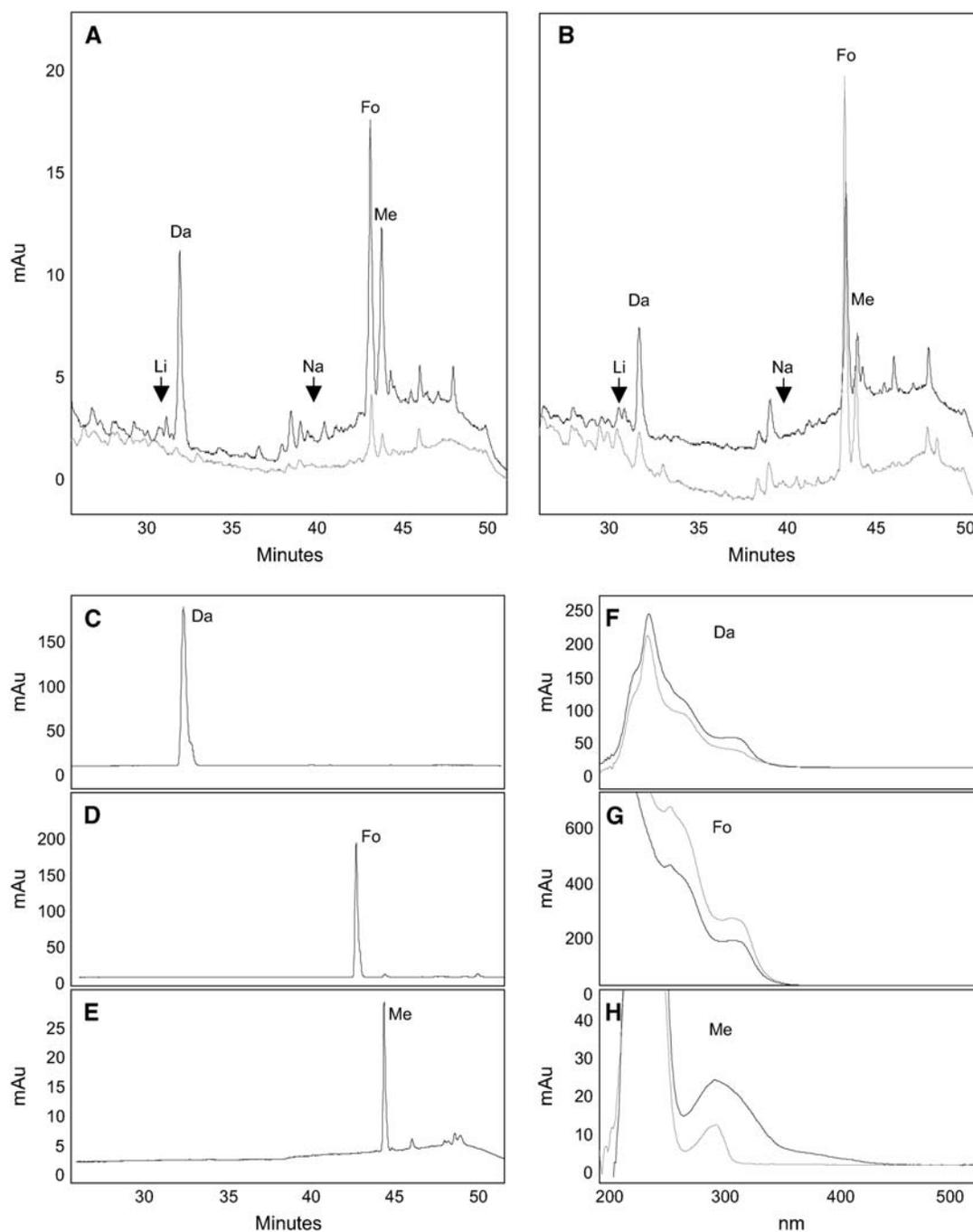
Phenotypic characterization of untreated control and CHS-silenced hairy roots showed no obvious differences. For all characterizations, only CHS-silenced hairy roots lacking blue intracellular fluorescence were analyzed. There were no statistically significant differences in the number of hairy roots formed per plantlet, the length of hairy roots, the width of hairy roots, the length of root hairs, or the number of emerged lateral roots per hairy root (Table 2).

To further investigate their ability to form nodules, we grew transformed control and CHS-silenced hairy root plantlets in Perlite in the presence of *S. meliloti*. The *S. meliloti* culture was supplemented with 2 μM of the flavone luteolin to ensure that *nod* gene expression in the rhizobia was stimulated even in the absence of flavonoids from the CHS-silenced hairy roots. After 3 weeks, control hairy root systems developed clearly visible

Figure 2. HPLC Chromatograms and Absorbance Spectra of Flavonoid Extracts from Roots.

All chromatograms show absorbance at 300 nm.
(A) Chromatograms of root extracts from empty vector control (black line; top) and CHS-silenced hairy roots (gray line; bottom) grown on Fåhraeus (F) medium. Daidzein (Da), formononetin (Fo), and medicarpin (Me) could be detected. Naringenin (Na) and liquiritigenin (Li) were below the detection limit. The gray and black lines were offset to make it easier to view both.
(B) Chromatograms of extracts from empty vector control (black line; top) and CHS-silenced roots (gray line; bottom) grown on medium complemented with 100 nM naringenin and 100 nM liquiritigenin in F medium. The gray and black lines were offset to make it easier to view both.
(C) to **(E)** Retention times of daidzein, formononetin, and medicarpin standards.
(F) to **(H)** Absorbance spectra of daidzein, formononetin, and medicarpin standards (gray lines) compared with the absorbance spectra of the respectively labeled peaks in (**[A]**; black lines).
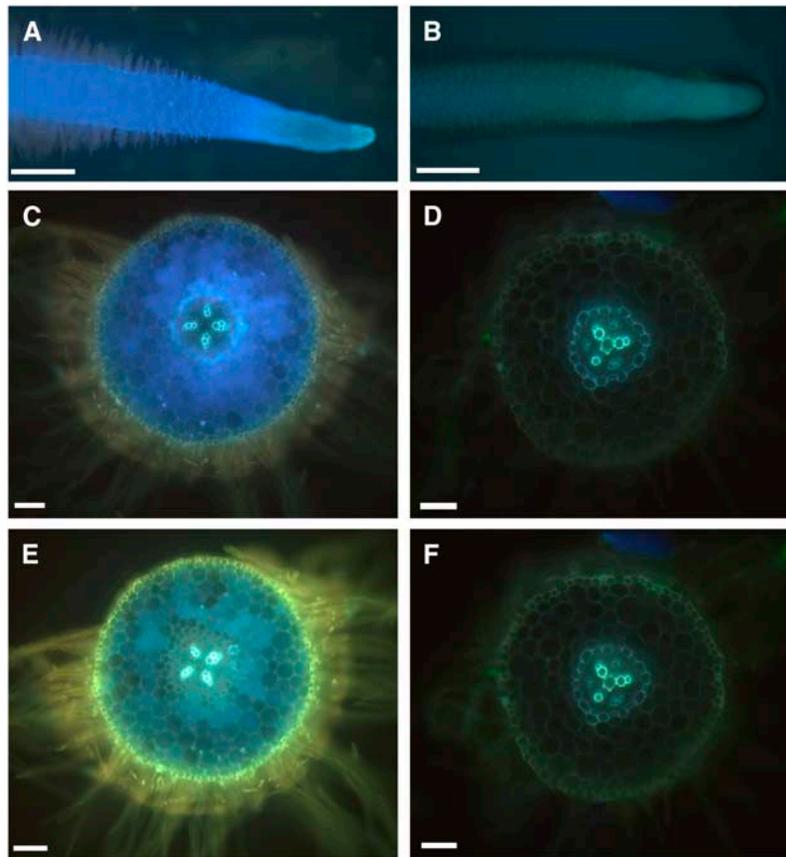
Figure 3. Fluorescence Microscopy of Control and CHS-Silenced Plants.

(A) Autofluorescence in a hairy root tip of a control hairy root.

(B) Autofluorescence in a hairy root tip of a CHS-silenced hairy root.

(C) Intracellular autofluorescence in a fresh vibratome section of a control hairy root.

(D) Autofluorescence in a fresh vibratome section of a CHS-silenced hairy root is limited to cell wall fluorescence.

(E) Enhanced and red-shifted intracellular and root hair fluorescence after addition of DPBA in a control hairy root section.

(F) No intracellular fluorescence is evident in a CHS-silenced hairy root section treated with DPBA.

(A) and **(B)**, **(C)** and **(E)**, and **(D)** and **(F)** were taken with the same exposure settings, respectively. Bars = 1 mm (**[A]** and **[B]**) and 100 μm (**[C]** to **[F]**).

nodules, whereas the nonfluorescent CHS-silenced root systems were devoid of nodules. Nodules only formed on CHS-silenced plants that still showed fluorescence and were before demonstrated to be not (fully) transformed (Table 2). As shown in Table 2, 28% of individual control hairy roots developed one or more nodules in this assay, with an average of ~0.5 nodules per individual hairy root (of the total numbers of roots, $n = 85$). Six percent of hairy roots on the CHS-silenced plants developed nodules ($n = 83$), but an examination of each of these nodules under UV light revealed strong blue intracellular fluorescence in these roots and their nodules, indicating that they had developed on untransformed hairy roots that escaped selection. No nodules were found on nonfluorescent hairy roots.

Nodulation experiments were repeated by growing hairy roots on agar plates and spot-inoculating roots with rhizobia. In a first experiment, rhizobia were not supplemented with luteolin; in a second independent experiment, rhizobia cultures were supplemented with 2 μM luteolin 12 h before inoculation. In both ex-

periments, nodules were formed on the empty vector control hairy roots, but significantly fewer ($P < 0.001$) nodules developed on CHS-silenced roots within 3 weeks (Table 2). Again, all nodules found on CHS-silenced roots showed blue fluorescence, indicating that these roots had escaped selection or were chimeric. We let the plants grow for a further 2 weeks but never observed nodules develop on CHS-silenced roots. While nodulation ability varied in the control hairy roots between experiments, there was no significant difference in the nodulation ability of plants inoculated with rhizobia in the presence or absence of luteolin.

To test at which stage of nodule development the CHS-silenced roots were affected, we used a GFP-labeled *S. meliloti* strain to localize the invading bacteria. Roots were spot-inoculated at the zone of emerging root hairs, and a 5-mm segment around the inoculation site was sectioned on a vibratome at 24 h, 48 h, 72 h, 5 d, and 10 d after inoculation. All roots were observed under UV light to test for the presence of flavonoids and under blue light to test for the presence of GFP-labeled rhizobia. The roots were

Table 2. Phenotypes of Empty Vector Control and CHS-Silenced Roots

Phenotype	Empty Vector Control (Mean ± SE)	CHS-Silenced (Mean ± SE)	P Level
Number of hairy roots per plantlet after 26 d	3.22 ± 0.27 ($n = 55$)	3.16 ± 0.33 ($n = 49$)	0.85
Hairy root length at 26 d (mm)	22.8 ± 2.07 ($n = 166$)	22.3 ± 2.18 ($n = 125$)	0.43
Hairy root width at 26 d, 1 cm behind root tip (mm)	1.08 ± 0.06 ($n = 40$)	1.10 ± 0.06 ($n = 40$)	0.35
Root hair length at 26 d (mm)	1.33 ± 0.04 ($n = 20$)	1.42 ± 0.04 ($n = 20$)	0.16
Number of lateral roots per root at 26 d	1.06 ± 0.13 ($n = 166$)	0.77 ± 0.14 ($n = 125$)	0.07
Number of nodules per root in Perlite (rhizobia grown with luteolin)	0.46 ± 0.06 ($n = 85$)	0.06 ± 0.02 ($n = 83$)[a]	<0.01
Number of nodules per root on agar (rhizobia grown without luteolin)	1.05 ± 0.29 ($n = 20$)	0.1 ± 0.05 ($n = 43$)[a]	<0.01
Number of nodules per root on agar (rhizobia grown with luteolin)	0.63 ± 0.13 ($n = 30$)	0.03 ± 0.01 ($n = 31$)[a]	<0.01
Number of nodules per complemented root on agar (rhizobia grown with luteolin)	0.76 ± 0.15 ($n = 39$)	0.60 ± 0.11 ($n = 35$)[a]	0.18

[a] All nodules found on CHS-silenced plantlets were located on roots that showed fluorescence in a screen for fluorescence at the end of the nodulation experiment.

then sectioned and stained with toluidine blue to visualize cell divisions. Root hair curling was observed on >90% of inoculated control (Figure 4A) and CHS-silenced hairy roots (Figure 4B) within 48 h. No root hair curling was observed on uninoculated roots. GFP-labeled rhizobia could be seen at the center of the curled root hairs and occasionally in infection threads. Cortical cell divisions (Figure 4C) and differentiating nodules were observed in 90% of spot-inoculated control hairy roots within 3 to 5 days but never in CHS-silenced roots.

To test whether the inability to nodulate was due to the absence of flavonoids or because of secondary effects of silencing CHS, we grew hairy roots on agar plates containing 100 nM naringenin and 100 nM liquiritigenin from the time of transformation. Naringenin is the product of chalcone isomerase and a precursor for the majority of flavonoids and has successfully been used to restore normal phenotypes to the *Arabidopsis* CHS mutant *tt4* (Shirley et al., 1995; Murphy et al., 2000). Liquiritigenin is a precursor of isoflavonoids, including daidzein, formononetin, and medicarpin (Jung et al., 2000; Winkel-Shirley, 2001). CHS-silenced roots, which were nonfluorescent on agar plates not containing naringenin and liquiritigenin (cf. Figure 3B), recovered blue intracellular fluorescence in 76% ($n = 108$) of hairy roots supplemented with flavonoids within 1 week, and this proportion of fluorescent roots was similar after 4 weeks (Figure 4D). When we extracted the supplemented roots and separated the flavonoids by HPLC, we could detect a very similar composition of flavonoids in the supplemented controls compared with unsupplemented empty vector controls (Figure 2B). No naringenin and liquiritigenin could be detected (Figure 2B), even though the detection limit for naringenin and liquiritigenin was 10^{-8} M, which was below the amounts (10^{-7} M) used in the supplementation medium (see Supplemental Figure 3 online). Complemented CHS-silenced roots showed higher levels of formononetin, daidzein, and medicarpin than nonsupplemented CHS-silenced roots, although the levels were only restored to ~30% (daidzein) to 50 to 100% (formononetin and medicarpin) of the control levels (Figure 2B). Nodule formation was restored in the supplemented CHS-silenced roots after inoculation of the roots with *S. meliloti* within 10 d (Figure 4E, Table 2). There was no significant difference (P = 0.18) in the numbers of nodules formed on supplemented empty vector control and supplemented CHS-

silenced roots (Table 2). Sectioning of these nodules (Figure 4G) showed that they had similar morphology and fluorescence characteristics to nodules on control hairy roots (Figure 4F). There was also no significant difference (P = 0.28) in the numbers of nodules formed on control hairy roots in the presence and absence of naringenin and liquiritigenin (Table 2). We also grew empty vector control and CHS-silenced hairy roots on naringenin- and liquiritigenin-supplemented medium for 4 weeks in the absence of rhizobia and did not observe any spontaneous nodules or other obvious phenotypes.

CHS-Silenced Hairy Roots Show Altered Auxin Transport

Auxin transport in *M. truncatula* roots was assessed by quantifying the amount of tritium-labeled indole-3-acetic acid (^{3}H-IAA) transported in the roots. As a positive test for inhibition of auxin transport in seedling root segments, we first applied NPA in small agar blocks at the zone of emerging root hairs 24 h prior to auxin transport measurements. ^{3}H-IAA was then applied in a small agar block positioned on the basipetal side of an excised root, 5 mm above the point of NPA application (see Supplemental Figure 4 online), and the auxin transported acropetally (from the ^{3}H-IAA source toward the root tip) into two 4-mm-long root sections, above and below the point of NPA application, was quantified. Application of NPA caused a significant (P < 0.05; $n = 20$) reduction in the amount of auxin transported acropetally in root segments (Figure 5A).

Comparison of auxin transport in untreated control and nonfluorescent CHS-silenced hairy roots showed significantly (P < 0.05; $n = 20$) higher rates of auxin transport in the flavonoid-deficient roots than in the control hairy roots (Figure 5B).

The ability of *S. meliloti* to alter auxin transport in control and nonfluorescent CHS-silenced roots was then assessed in 20 hairy roots for each treatment, using NPA as a positive control and mock-inoculated roots as a negative control (Figure 5C). Transport capacity was assessed 24 h after inoculation, since previous experiments in the lab showed that auxin transport inhibition following *S. meliloti* inoculation in *M. truncatula* was greatest after ~24 h (data not shown). In the section above the point of treatment, neither NPA nor *S. meliloti* inoculation significantly affected auxin transport in control or CHS-silenced roots,
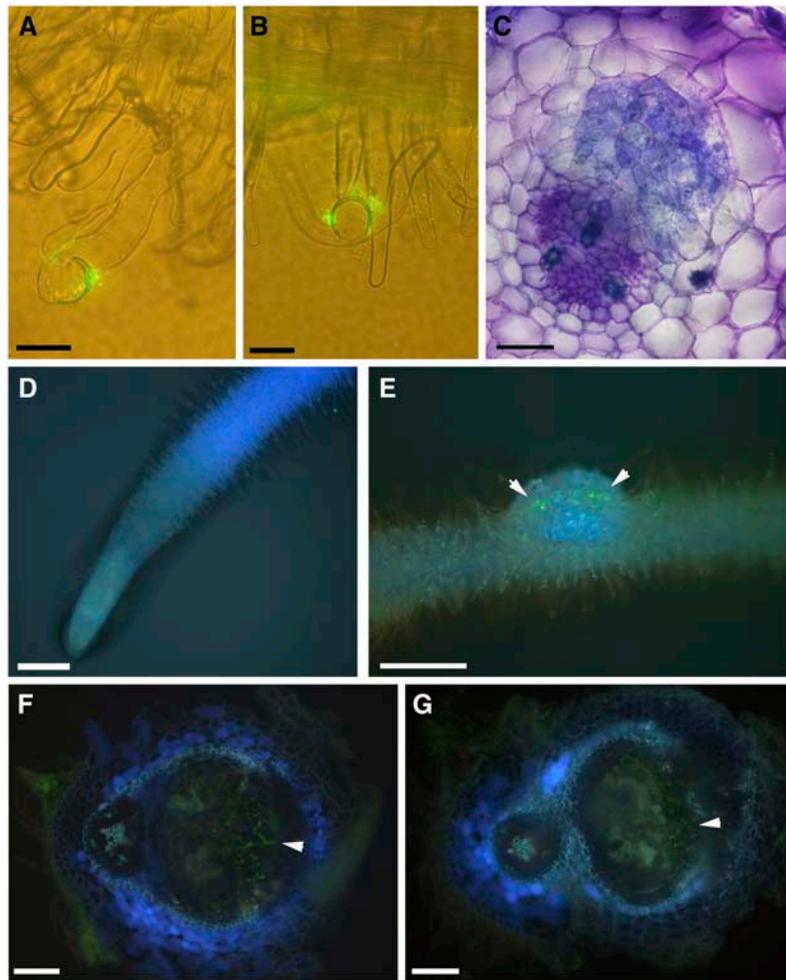
Figure 4. Effects of Flavonoid Deficiency on Nodulation.

(A) Root hair curling on a control hairy root 48 h after inoculation with GFP-labeled *S. meliloti*.

(B) Root hair curling on a CHS-silenced hairy root 48 h after inoculation with GFP-labeled *S. meliloti*.

(C) Cortical cell divisions in control hairy roots 72 h after inoculation, stained with toluidine blue.

(D) Autofluorescence in a CHS-silenced root grown for 1 week on flavonoid-supplemented medium. This photo was taken at the same time with the same exposure settings as Figures 3A and 3B.

(E) Nodule developing on a CHS-silenced root grown on flavonoid-supplemented medium 10 d after inoculation with GFP-labeled *S. meliloti*, which can be seen on the nodule surface (arrowheads).

(F) Autofluorescence of a fresh vibratome section of a 10-d-old nodule of a control hairy root grown on flavonoid-supplemented medium. Infection threads of GFP-labeled bacteria can be seen at the arrowhead.

(G) Autofluorescence of a fresh vibratome section of a 10-d-old nodule of a CHS-silenced hairy root grown on flavonoid-supplemented medium. Infection threads of GFP-labeled bacteria can be seen at the arrowhead.

Bars = 50 μm (**[A]** and **[B]**), 100 μm **(C)**, 1 mm (**[D]** and **[E]**), and 500 μm (**[F]** and **[G]**).

but auxin transport was significantly higher in the CHS-silenced roots ($P < 0.05$) than in control roots. In the section below the point of treatment, both NPA and *S. meliloti* inoculation significantly ($P < 0.05$) reduced auxin transport in control hairy roots. By contrast, *S. meliloti* inoculation of CHS-silenced hairy roots did not reduce auxin transport, whereas NPA treatment did ($P < 0.001$). These results showed that (1) CHS-silenced roots were not defective in auxin transport regulation by auxin transport inhibitors per se, (2) *S. meliloti* inoculation caused auxin transport

inhibition in control hairy roots, and (3) the ability of *S. meliloti* to inhibit auxin transport was flavonoid dependent.

To test whether the effect of flavonoids on auxin transport was due to changes in the expression of the *PIN* genes, we monitored the mRNA levels of all 10 known *M. truncatula PIN* genes from *M. truncatula* (Schnabel and Frugoli, 2004) using semiquantitative RT-PCR. A comparison of transcript levels of control and CHS-silenced hairy roots showed no observable differences in the levels of *PIN1*, *PIN2*, *PIN3*, *PIN4*, *PIN6*, *PIN7*, *PIN9*, and *PIN10*.
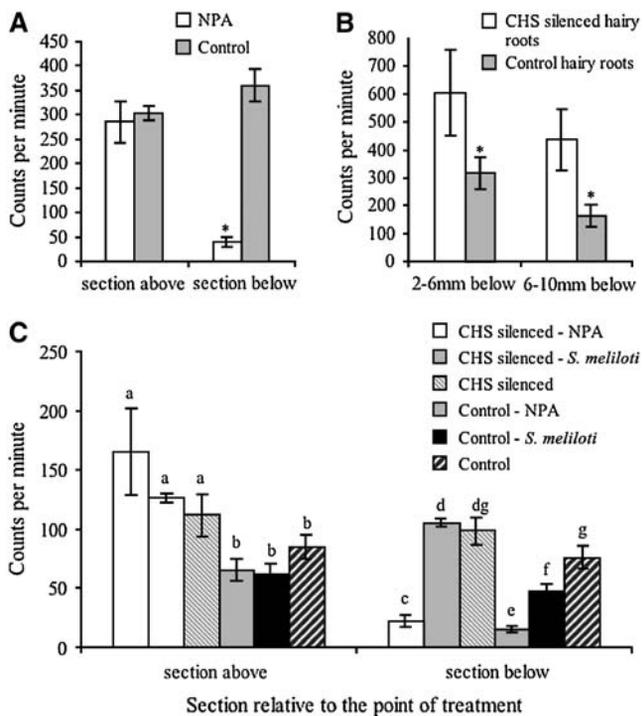
Figure 5. Acropetal Auxin Transport Measurements in Hairy Roots.

(A) Effect of 24 h treatment with NPA on auxin transport in control seedling roots. The asterisk indicates a significant difference at the 0.01 level in the NPA treatment compared with control (Student's t test; $n = 10$).

(B) Comparison of auxin transport in untreated control and CHS-silenced hairy roots. The asterisk indicates a significant difference at the 0.05 level in the CHS-silenced roots compared with control roots (Student's t test; $n = 19$ to 20).

(C) Effect of *S. meliloti* and NPA on auxin transport in control and CHS-silenced hairy roots. Any two pairwise comparisons of treatments labeled with different letters are significantly different from each other at the 0.05 level (one way analysis of variance; $n = 10$ to 24).

All error bars indicate standard errors of the mean. For the experimental setup, see Supplemental Figure 4 online.

The transcript levels for *PIN5* and *PIN8* were almost undetectable (data not shown).

DISCUSSION

Silencing of CHS in *M. truncatula* Leads to Deficiency in Flavonoids in Hairy Roots

We used *A. rhizogenes* transformation to express a *CHS* ihpRNA construct, thus silencing the flavonoid pathway in *M. truncatula* roots. Because it is not known which flavonoids in legumes could act as auxin transport regulators during nodulation, we focused on silencing CHS, which catalyzes the first committed step of the flavonoid pathway, to generate flavonoid deficient roots. RT-PCR confirmed that transcript levels were reduced significantly, in most cases to undetectable levels, when compared with con-

trol levels. RNAi typically produces dramatically reduced but detectable levels of target gene activity (Wesley et al., 2001). This would account for the small amount of CHS transcript still detectable in some CHS-silenced hairy roots. The 75% cotransformation efficiency measured in this approach compares well with the previously reported efficiencies of ~70% (Boisson-Dernier et al., 2001) and 85% (Limpens et al., 2004) in *M. truncatula* hairy roots. In our plantlets, RNAi appeared to be restricted to the hairy roots only. This nonsystemic silencing using RNAi in *M. truncatula* hairy roots was also observed by Limpens et al. (2004), whereas hairy root plantlets of other species of legumes, including *L. japonicus* (Kumagai and Kouchi, 2003) and soybean (Subramanian et al., 2005), showed systemic silencing to the shoot.

The use of intracellular fluorescence loss as a marker of CHS silencing in hairy roots is consistent with the absence of fluorescence in the *Arabidopsis* CHS mutant *tt4* (Shirley et al., 1995; Peer et al., 2001; Buer and Muday, 2004). The presence of blue fluorescence in root tips and cortical cells and fluorescence in root hairs correlates with the expression of *CHS* in those tissues in *M. truncatula* (Harrison and Dixon, 1994). The shift of fluorescence induced by DPBA was an additional indication that the fluorescence was due to flavonoids. DPBA is a reagent that indicates the presence of many flavonoids through a bathochromic shift and intensification of fluorescence (Neu, 1956; Homberg and Geiger, 1980; Markham, 1982), although it can also stain some anthraquinones (aloin and aloinosides) (Wagner et al., 1984). It has been used in many studies to detect flavonoids in plant tissues (Sheahan and Rechnitz, 1992; Vogt et al., 1994; Hutzler et al., 1998). Furthermore, no fluorescence was detected when staining the flavonoid-deficient *Arabidopsis tt4* mutant with DPBA (Peer et al., 2001). We have confirmed the correlation of silencing and fluorescence loss using RT-PCR to profile *CHS* expression in individual hairy roots from a sample set of our control and CHS-silenced hairy roots. Thus, fluorescence is an appropriate marker of *CHS* expression and allows us to detect hairy roots that have been successfully transformed.

HPLC and TLC confirmed that flavonoid content was significantly reduced in the CHS-silenced roots. Small amounts of flavonoids were still present and could have been due to flavonoids in untransformed or chimeric roots, which may have escaped screening to be mixed in with transformed roots before the extraction. We identified the isoflavonoids daidzein, formononetin, and medicarpin as the most abundant flavonoid aglycones in *M. truncatula* roots, although others may have been present at low levels. These isoflavonoids and their glycosides have previously been identified in *M. truncatula* roots (Harrison and Dixon, 1993; Baggett et al., 2002).

We have therefore concluded that RNAi of *CHS* in *M. truncatula* resulted in transformed hairy roots largely deficient in flavonoids. The complementation of the nodulation and flavonoid deficiency in roots by the external addition of naringenin and liquiritigenin suggests that the lack of flavonoids was the reason for nodulation deficiency and the absence of intracellular fluorescence in the roots. Since no naringenin and liquiritigenin were detected in the complemented roots, the addition of these flavonoid precursors most likely resulted in metabolic conversion to the usual end products found in *M. truncatula*.

Flavonoid Deficiency Prevents the Formation of Root Nodules

Flavonoids could play a number of different roles in legumes during nodule development. Their role as *nod* gene inducers and as a chemotactic signal to rhizobia in the soil has been studied previously (Redmond et al., 1986; Djordjevic et al., 1987; Peters and Long, 1988). In our experiments, we added the *nod* gene inducer luteolin to *S. meliloti* cultures to control for adequate expression of *nod* genes (Peters et al., 1986). The inability of CHS-silenced roots to nodulate was irrespective of the addition of luteolin to the rhizobial culture (Table 2). It is therefore unlikely that the absence of nodules was due to the inability of the rhizobia to form Nod factors. This was also suggested by the ability of the inoculated rhizobia to cause normal root hair curling, a Nod factor–dependent phenotype, on the CHS-silenced hairy roots (Figure 4B). However, we cannot exclude the possibility that the absence of root flavonoids prevented sustained Nod factor production inside the root, which might be necessary for nodule initiation.

In addition to their activity as *nod* gene inducers, flavonoids could have roles as developmental signals (Hirsch, 1992; Spaink, 1998). Flavonoids are specifically induced in the precursor cells of a nodule primordium and later also found in dividing cells of the nodule in white clover (Mathesius et al., 1998b). In this study, we found nodules and nodule primordia to always contain intracellular fluorescence (Figures 4E to 4G) and never observed nodules on nonfluorescent roots of CHS-silenced plants. The application of naringenin and liquiritigenin rescued the formation of nodules on CHS-silenced hairy roots (Figure 4E, Table 2), supporting our central hypothesis that flavonoids are necessary for the initiation of nodules in *M. truncatula*.

Auxin Transport Regulation Is Defective in CHS-Silenced Roots

Flavonoids have long been hypothesized to act as auxin transport inhibitors and, thus, regulators of plant development (Stenlid, 1976; Jacobs and Rubery, 1988). Our results showed further that flavonoid deficiency in roots increased auxin transport (Figure 5B). This agrees with evidence of increased auxin transport in the *Arabidopsis* flavonoid deficient *tt4* mutant (Murphy et al., 2000; Brown et al., 2001; Buer and Muday, 2004). Increased auxin transport did not appear to be due to altered sensitivity to NPA, as NPA-treated CHS-silenced hairy roots showed similar reduction in auxin transport to control hairy roots (Figure 5C). Comparable results were found in the *Arabidopsis tt4* mutant (Brown et al., 2001).

Since the discovery that auxin transport inhibitors can induce pseudonodules in legumes (Allen et al., 1953; Hirsch et al., 1989), it has been suggested that flavonoids could be the signals that regulate auxin transport during nodulation. This hypothesis has been difficult to test for the lack of flavonoid-deficient legume mutants. Our results showed that inoculation with rhizobia reduced auxin transport in control hairy roots but that this ability was inhibited in roots lacking flavonoids (Figure 5C). This provides genetic evidence for the hypothesis that flavonoids act as auxin transport regulators during nodule organogenesis. Our results support previous evidence in white clover, which showed that

flavonoid aglycones induce similar changes in auxin transport inhibition as rhizobia or their Nod factors (Mathesius et al., 1998a). The results also support experiments by Boot et al. (1999) that showed that nodulating rhizobia and their Nod factors inhibit auxin transport capacity. So far it is not clear which flavonoids act as auxin transport regulators in legumes or how they act, and their identity will need to be determined in future studies. None of the flavonoids identified in *M. truncatula* in this study necessarily have to be the auxin transport inhibitor associated with nodulation because the auxin transport inhibitors are most likely locally and transiently induced by rhizobia.

In white clover, flavonoids are colocated with *GH3:GUS* expression within nodules and their primordia (Mathesius et al., 1998b, 1998a). Nodule primordia also express the gene for the auxin import carrier AUX1, and it has been suggested that this allows the channeling of auxin to a newly initiated nodule primordium (de Billy et al., 2001). It is possible that flavonoids act locally in cells that require redirection of auxin transport and accumulation to allow new cell division and differentiation to proceed. Detailed analyses of flavonoid action in the *Arabidopsis tt4* mutant have revealed that auxin export by members of the PIN family is not only regulated by flavonoids but also by auxin transport rates per se (Peer et al., 2004). In addition, the accumulation of flavonoids is auxin regulated, suggesting a feedback loop between auxin transport rates, flavonoid accumulation, and the action of flavonoids on further auxin transport. Flavonoids and other auxin transport inhibitors have been shown to act on the cycling of the PIN transporter between the plasma membrane and endosomal vesicles in *Arabidopsis* root tips (Geldner et al., 2001; Peer et al., 2004). In *Arabidopsis*, it has also been shown that flavonoids affect the expression of *PIN1* and *PIN2* and that varying auxin transport by applying NPA can also affect *PIN* expression (Peer et al., 2004). We did not find any evidence of altered *PIN* expression in hairy roots of control and CHS silenced plants, even though their auxin transport capacity differed. It is possible that *PIN* expression is regulated differently in *M. truncatula* compared with *Arabidopsis*, for example, if flavonoids act mainly posttranscriptionally to alter PIN activity or cycling.

Interestingly, the CHS-silenced hairy roots showed no significant alteration in the frequency of lateral root formation. This is in contrast with the flavonoid-deficient *Arabidopsis tt4* mutant, which showed increased numbers of lateral roots (Brown et al., 2001). In *Arabidopsis*, a strong correlation has been demonstrated between auxin transport and lateral root formation. For example, lateral root formation is reduced after inhibition of auxin transport (Reed et al., 1998) and promoted after increases in auxin transport (Casimiro et al., 2001). *Arabidopsis PIN* mutants were shown to be defective in auxin transport (Gälweiler et al., 1998), auxin localization in lateral root primordial, and the correct formation of lateral organs (Benková et al., 2003). It is possible that the increase in auxin transport in *M. truncatula* CHS-silenced roots was not severe enough to increase lateral root formation, that the composite nature of hairy root plantlets affected shoot-derived auxin, or that legumes in general might have different requirements for auxin transport in respect to lateral root formation than *Arabidopsis*.

In addition to the role of flavonoids in nodule formation in legumes, it has also been suggested that flavonoids play a role as

auxin transport regulators during *Agrobacterium tumefaciens*–induced tumor formation (Schwalm et al., 2003) and root knot nematode-induced gall formation (Hutangura et al., 1999). The flavonoid-deficient *M. truncatula* hairy roots could be used in the future to test the role of flavonoids in these interactions.

METHODS

Bacterial Strains

GFP-labeled *Sinorhizobium meliloti* strain 1021 (Gage et al., 1996) was maintained on Bergensen's modified medium (Rolfe et al., 1980) plates containing 50 μM tetracycline. *Agrobacterium rhizogenes* ARqua1 strain (Boisson-Dernier et al., 2001) was maintained on tryptone yeast medium containing 100 μg/mL streptomycin.

Generation of CHS RNAi Vector and Transformation of *A. rhizogenes*

The RNAi vector used to silence CHS transcripts was constructed as follows. The sequence coding for putative CHS (chs1) mRNA in *Medicago truncatula* (AJ277211.1) was downloaded from GenBank and was used to identify 14 homologous tentative consensus sequences from the TIGR Unique Gene Indices (www.tigr.org) for *M. truncatula* using BLASTN: (TC106537, TC106536, TC106539, TC106544, TC106552, TC106554, TC102579, TC106549, TC106538, TC95902, TC105903, TC106550, TC106555, and TC106559). These sequences were aligned (prodes. toulouse.inra.fr/multalin/multalin.html), and a conserved 543-bp region toward the 5′ end (showing 88.2% identity between AJ277211.1 and the consensus sequence from the alignment) was amplified by RT-PCR using primers modified with attB recombinase sites (Invitrogen). The forward primer sequence was 5′-GGGGACAAGTTTGTACAAAAAAGCAGGCCG-TAAAGCTCAAAGGGCAGA-3′ (attB1 site underlined), and the reverse primer sequence was 5′-GGGGACCACTTTGTACAAGAAAGCTGGG-TAACCAACACACGAGCACCTT-3′ (attB2 site underlined). Total RNA from *M. truncatula* was isolated with the RNeasy plant mini kit from Qiagen, and RT-PCR was performed using the SuperScript one-step RT-PCR kit. The PCR product was recombined into pDONR201 and then pHellsgate8 (a kind gift of Peter Waterhouse, CSIRO Plant Industry, Canberra, Australia). Recombination reactions were performed according to the manufacturer's protocol (Invitrogen).

The vectors were screened for by restriction digests and verified by sequencing. After sequencing, the pHellsgate8-CHS vector was transformed into the *A. rhizogenes* ARqua1 strain (provided by Karam Singh, CSIRO Plant Industry, Perth, Australia) using the freeze-thaw transformation method from Hofgen and Willmitzer (1988).

Hairy Root Transformation and Plant Growth Conditions

M. truncatula cv Jemalong A17 seeds were scarified on sandpaper, sterilized in 6% hypochlorite for 10 min, and thoroughly rinsed in sterile water. Seeds were vernalized at 4°C overnight and then germinated at 25°C in the dark on inverted agar plates. The transformation of *M. truncatula* with *A. rhizogenes* followed the technique of Boisson-Dernier et al. (2001). Transformation with empty pHellsgate8 vector was used throughout the study as a negative control. For nodulation experiments, NH_4NO_3 was omitted from the media and agar was replaced by Phytagel (Sigma-Aldrich). Hairy root plantlets were grown in a growth chamber at 25°C, with a 16-h light period at 150 μE light intensity. For phenotypic characterizations, plantlets were grown for 4 weeks on 15-cm-diameter Petri dishes containing sloped modified F medium (Boisson-Dernier et al., 2001). All roots were tested for the presence of flavonoid fluorescence (see Microscopy section). Measurements of root width and root hair length were made in the mature root at 1 cm distance from the root tip under a light microscope containing a graticule.

Semiquantitative RT-PCR

Hairy root RNA was prepared with the RNeasy plant RNA extraction kit (Qiagen) and was converted to cDNA with the SuperScript first strand synthesis system for RT-PCR (Invitrogen) according to the manufacturer's protocol. The cDNA was then diluted to fixed quantities (50 to 100 ng/μL) and gene expression compared using PCR. PCR reactions were performed in a Biometra T3 thermocycler PCR machine using 28 to 30 cycles of 94°C for 30 s, 50°C for 30 s, and 72°C for 1 min. The 20-μL reaction volumes were used (2 μL 10× buffer, 0.6 μL 50 mM MgCl$_2$, 0.4 μL 10 mM deoxynucleotide triphosphate mix, 0.4 μL 0.2 μM forward primer, 0.4 μL 0.2 μM reverse primer, 0.2 μL Taq, 15 μL deionized water, and 1 μL cDNA [components from Invitrogen]).

The *M. truncatula* actin gene (TC107326) was used as a control. The following primer pairs were used to amplify the actin and CHS fragments, respectively: 5′-GCTGTCCTCTCCCTCTATGC-3′ and 5′-CAATGTTGC-CGTACAGATCC-3′; 5′-CGCTGTCACATTTCGTGG-3′ and 5′-AACAC-ACCCCATTCAAGTCC-3′.

The primers for the *M. truncatula CHS* sequence amplified a conserved region separate to the region targeted for RNAi, thus avoiding competitive binding with ihpRNA. They are expected to amplify all *CHS* sequences targeted by the RNAi construct. Primers used for the 10 *M. truncatula PIN* genes were as described by Schnabel and Frugoli (2004).

HPLC

One-week-old roots of control or CHS-silenced hairy root plantlets were excised from the plants, immediately ground in liquid nitrogen with a mortar and pestle, and weighed into an Eppendorf tube. Approximately 10 to 20 roots were pooled for each extraction after screening for root fluorescence. Per 100 mg of fresh weight, 300 μL 100% HPLC-grade acetone was used to extract flavonoids. After centrifugation, the supernatant was dried down, and the remnant redissolved in 2 M HCl:100% methanol (1:1) and boiled in a water bath for 1 h to hydrolyze flavonoid glycosides (Markham, 1989). After drying down the mixture, 1:1 water: ethyl acetate was added to a final volume equal to the original volume of acetone. After vigorous shaking, the ethyl acetate phase was collected and dried down, and aglycones were redissolved in an equal volume of acetone. Flavonoids were separated on a Shimadzu LC-10 VP series HPLC, equipped with a diode array UV/VIS detector and a fluorescence detector, using an Alltec Altima C18 5u reverse phase column (250 × 4 mm; Alltech Associates) with the following gradient. Solvent A was Milli-Q purified water, and solvent B was HPLC-grade acetonitrile (Lab Scan Analytical Sciences): 0 to 2 min 10% B, 2 to 35 min linear gradient from 10 to 40% B, 35 to 45 min linear gradient from 40 to 80% B, 45 to 47 min 80% B, 47 to 52 min linear gradient from 80 to 10% B, and 52 to 60 min 10% B. The flow rate was 1 mL per minute. Absorbance was recorded between 190 and 700 nm, and fluorescence emission was detected at 450 nm (excitation at 365 nm). For determination of relative abundance of the compounds, peak areas were integrated using the Shimadzu software. To identify the separated peaks, a number of standard flavonoids and precursors, dissolved at 1 to 10 mM in acetone, were separated under the same conditions, including naringenin, naringin, genistein, genistin, daidzein, *p*-coumaric acid, apigenin, quercitin, quercitrin, luteolin (Sigma-Aldrich), 7,4′-dihydroxyflavone, ononin, liquiritigenin, ferulic acid, 6-OH flavone (Indofine Chemical Company), formononetin, kaempferol, coumestrol, biochanin A (Fluka Chemie), and medicarpin (Sequoia Research Products). HPLC of flavonoid extracts was performed four times each in control and CHS-silenced roots, using different batches of transformed plants. All batches yielded similar results.

TLC

Roots were extracted as for the HPLC separation. Fifty microliters of extract of both empty vector control roots and CHS-silenced roots, adjusted to the same amount of acetone per fresh weight of roots, were spotted onto nonfluorescent silica-coated TLC plates (Merck). All standards used for HPLC were also used for TLC. Extracts were separated in hexane:isopropanol:methanol:water (100:12:0.3:0.3). Plates were viewed under a UV lamp (maximum excitation 365 nm) and photographed with a digital camera (Kodak EasyShare DX4330).

Nodulation Studies

One-week-old composite plantlets were transferred to pots (50 mL volume) containing Perlite soaked in liquid F medium (Fåhraeus, 1957) and were kept moist with sterile Milli-Q water. GFP-labeled *S. meliloti* strain 1021 was inoculated into liquid BMM and grown overnight to an OD_{600} of 0.2 (28°C at 180 rpm), supplemented with 2 μM luteolin where stated (Sigma-Aldrich). Five milliliters of culture was pipetted onto the root system of each plantlet. After 3 weeks, the seedlings were carefully removed from the pots and the number of nodules on the root system counted under a stereomicroscope. Nodulation was also performed on nitrogen-free F medium containing Phytagel (Sigma-Aldrich) as the gelling agent. For complementation assays, nodulation of transformed hairy roots was performed on F medium that was supplemented with 100 nM naringenin and 100 nM liquiritigenin. For all plate assays, roots were spot-inoculated by placing ~1 μL of bacterial culture (including 2 μM luteolin where stated) at the zone of emerging root hairs using a glass capillary pulled over a flame and glued to a hypodermic needle that was attached to a syringe.

Microscopy

Roots were cut into 5-mm segments and immediately embedded in 3% DNA-grade agarose (Progen Biosciences). They were then cross-sectioned at 150-μm thickness on a vibratome (1000 plus; Vibratome Company). The thickness of the sections was chosen to ensure that vacuole contents of cells were retained. Cytoplasmic streaming could be observed in cells after sectioning, confirming that cell contents were retained. Sections were transferred to glass slides, kept under a cover slip in distilled water, and viewed immediately under an epifluorescence microscope (Leica DMLB) using a UV excitation filter (excitation maximum at 365 nm; 425-nm long-pass filter). Images were taken with a mounted CCD camera (RT Slider; Diagnostic Instruments). Flavonoids were stained by incubating fresh sections for 5 min in DPBA (Sigma-Aldrich) (0.5% in 10 mM phosphate buffer, 2% DMSO, and 1% sucrose, pH 6) (Sheahan and Rechnitz, 1992). Images were taken before and after staining with the same exposure settings and the fluorescence compared. To visualize GFP-labeled bacteria, sections were viewed using a blue excitation filter (excitation maximum 488 nm; 515-nm long-pass filter). Toluidine blue staining was done by incubating sections for 5 min in 0.5% toluidine blue, pH 4.4, washing sections with distilled water, and viewing under bright-field illumination.

Auxin Transport Measurements

Prior to auxin transport measurements, roots were treated by spot-inoculation of rhizobia or by placing a small agar block ($2 \times 2 \times 5$ mm^3) containing an auxin transport inhibitor (1 mM NPA) or solvent controls (at equal concentrations) at the zone of emerging root hairs (see Supplemental Figure 4 online). ^{3}H-IAA solution (7.5 μL of 1 mCi/mL; Amersham Biosciences) was diluted in 30 μL of ethanol and mixed into 1.5 mL of melted and cooled 4% agarose (Amresco), ~pH 4.8, in a sterile Petri dish. Once solid, the agar was cut into $2 \times 2 \times 2$-mm^3 donor blocks. Initial experiments on seedling roots showed that basipetal auxin transport

resulted in <10% of acropetal auxin transport at the zone of root hair emergence (data not shown), confirming that the majority of auxin is transported acropetally in this part of the root. Similar results have been reported from *Arabidopsis thaliana* (Rashotte et al., 2003). Therefore, all subsequent auxin transport experiments were conducted by measuring acropetal auxin transport. Plant roots were cut 5 mm basipetal from the point of spot inoculation or treatment. The roots were then laid on a modified F plate with the basipetal (cut) end in contact with a donor block and separated from the media by a strip of Parafilm (to prevent diffusion of the ^{3}H-IAA through the agar). The plates were placed vertically in a box and covered with aluminum foil. They were incubated at room temperature for 12 h. The roots were then cut into two 4-mm segments, above and below the point of treatment, after removal of the first millimeter of root in contact with the donor block, and each placed into a scintillation vial containing 4.5 mL of scintillation fluid (Perkin-Elmer). The vials were shaken overnight and radioactivity counted in a scintillation counter (Beckman Coulter LS6500) over 3 min. Previous experiments in our lab have shown that almost all of the radioactivity recovered from roots in these assays is still associated with IAA extracted from the roots (van Noorden et al., 2006). Donor blocks were also counted to test for variability in auxin amounts of the blocks.

Statistical Analysis

Analysis of variance was calculated using Genstat for Windows (version 5.0; Rothamsted Agricultural Trust). Student's *t* tests were performed using Microsoft Excel 2002.

Accession Numbers

Sequence data on the *CHS* genes targeted in our silencing approach can be found at GenBank (accession number AJ277211.1) and at the TIGR *M. truncatula* gene index (http://www.tigr.org/tigr-scripts/tgi/T_index.cgi?species=medicago) (tentative consensus sequence numbers TC106537, TC106536, TC106539, TC106544, TC106552, TC106554, TC102579, TC106549, TC106538, TC95902, TC105903, TC106550, TC106555, and TC106559).

Supplemental Data

The following materials are available in the online version of this article.

    Supplemental Figure 1. Fluorescence Chromatogram of Control and CHS-Silenced Hairy Root Extracts.

    Supplemental Figure 2. TLC Plate of Control and CHS-Silenced Hairy Root Extracts (Not Hydrolyzed).

    Supplemental Figure 3. Retention Times of Standards of Liquiritigenin, Naringenin, Ononin (Formononetin-7-*O*-β-D-Glucopyranoside), and Coumestrol.

    Supplemental Figure 4. Schematic Setup for Auxin Transport Experiments.

    Supplemental Figure 5. Fluorescence Chromatogram of Medicarpin Standard.

REFERENCES

Allen, E.K., Allen, O.N., and Newman, A.S. (1953). Pseudonodulation of leguminous plants induced by 2-bromo-3,5-dichlorobenzoic acid. Am. J. Bot. **40,** 429–435.

Ane, J.M., et al. (2004). *Medicago truncatula* DMI1 required for bacterial and fungal symbioses in legumes. Science **303,** 1364–1367.

Baggett, B.R., Cooper, J.D., Hogan, E.T., Carper, J., Paiva, N.L., and Smith, J.T. (2002). Profiling isoflavonoids found in legume root extracts using capillary electrophoresis. Electrophoresis **23,** 1642–1651.

Benková, E., Michniewicz, M., Sauer, M., Teichmann, T., Seifertova, D., Jürgens, G., and Friml, J. (2003). Local, efflux-dependent auxin gradients as a common module for plant organ formation. Cell **115,** 591–602.

Bennett, M.J., Marchant, A., May, S.T., and Swarup, R. (1998). Going the distance with auxin: Unravelling the molecular basis of auxin transport. Philos. Trans. R. Soc. Lond. B Biol. Sci. **353,** 1511–1515.

Boisson-Dernier, A., Chabaud, M., Garcia, F., Becard, G., Rosenberg, C., and Barker, D.G. (2001). *Agrobacterium rhizogenes*-transformed roots of *Medicago truncatula* for the study of nitrogen-fixing and endomycorrhizal symbiotic associations. Mol. Plant Microbe Interact. **14,** 695–700.

Boot, K.J.M., van Brussel, A.A.N., Tak, T., Spaink, H.P., and Kijne, J.W. (1999). Lipochitin oligosaccharides from *Rhizobium leguminosarum* bv. *viciae* reduce auxin transport capacity in *Vicia sativa* subsp *nigra* roots. Mol. Plant Microbe Interact. **12,** 839–844.

Brown, D.E., Rashotte, A.M., Murphy, A.S., Normanly, J., Tague, B.W., Peer, W.A., Taiz, L., and Muday, G.K. (2001). Flavonoids act as negative regulators of auxin transport in vivo in Arabidopsis. Plant Physiol. **126,** 524–535.

Buer, C.S., and Muday, G.K. (2004). The transparent testa4 mutation prevents flavonoid synthesis and alters auxin transport and the response of Arabidopsis roots to gravity and light. Plant Cell **16,** 1191–1205.

Casimiro, I., Marchant, A., Bhalerao, R.P., Beeckman, T., Dhooge, S., Swarup, R., Graham, N., Inzé, D., Sandberg, G., Casero, P.J., and Bennett, M. (2001). Auxin transport promotes Arabidopsis lateral root initiation. Plant Cell **13,** 843–852.

de Billy, F., Grosjean, C., May, S., Bennett, M., and Cullimore, J.V. (2001). Expression studies on AUX1-like genes in *Medicago truncatula* suggest that auxin is required at two steps in early nodule development. Mol. Plant Microbe Interact. **14,** 267–277.

Dénarié, J., and Debellé, F. (1996). *Rhizobium* lipo-chitooligosaccharide nodulation factors: Signaling molecules mediating recognition and morphogenesis. Annu. Rev. Biochem. **65,** 503–535.

Djordjevic, M.A., Mathesius, U., Arioli, T., Weinman, J.J., and Gartner, E. (1997). Chalcone synthase gene expression in transgenic subterranean clover correlates with localised accumulation of flavonoids. Aust. J. Plant Physiol. **24,** 119–132.

Djordjevic, M.A., Redmond, J.W., Batley, M., and Rolfe, B.G. (1987). Clovers secrete specific phenolic compounds which either stimulate or repress *nod* gene expression in *Rhizobium trifolii*. EMBO J. **6,** 1173–1179.

Fåhraeus, G. (1957). The infection of clover root hairs by nodule bacteria studied by a simple glass slide technique. J. Gen. Microbiol. **16,** 374–381.

Gage, D.J., Bobo, T., and Long, S.R. (1996). Use of green fluorescent protein to visualize the early events of symbiosis between *Rhizobium meliloti* and alfalfa (*Medicago sativa*). J. Bacteriol. **178,** 7159–7166.

Gälweiler, L., Guan, C.H., Muller, A., Wisman, E., Mendgen, K., Yephremov, A., and Palme, K. (1998). Regulation of polar auxin transport by AtPIN1 in Arabidopsis vascular tissue. Science **282,** 2226–2230.

Geldner, N., Friml, J., Stierhof, Y.D., Jürgens, G., and Palme, K. (2001). Auxin transport inhibitors block PIN1 cycling and vesicle traficking. Nature **413,** 425–428.

Harrison, M.J., and Dixon, R.A. (1993). Isoflavonoid accumulation and expression of defense gene transcripts during the establishment of vesicular-arbuscular mycorrhizal associations in roots of *Medicago truncatula*. Mol. Plant Microbe Interact. **6,** 643–654.

Harrison, M.J., and Dixon, R.A. (1994). Spacial patterns of expression of flavonoid/isoflavonoid pathway genes during interactions between roots of *Medicago truncatula* and the mycorrhizal fungus *Glomus versiforme*. Plant J. **6,** 9–20.

Hirsch, A.M. (1992). Developmental biology of legume nodulation. New Phytol. **122,** 211–237.

Hirsch, A.M., Bhuvaneswari, T.V., Torrey, J.G., and Bisseling, T. (1989). Early nodulin genes are induced in alfalfa root outgrowths elicited by auxin transport inhibitors. Proc. Natl. Acad. Sci. USA **86,** 1244–1248.

Hofgen, R., and Willmitzer, L. (1988). Storage of competent cells for *Agrobacterium transformation*. Nucleic Acids Res. **16,** 9877.

Homberg, H., and Geiger, H. (1980). Fluoreszenz und struktur von flavonen. Phytochem. **19,** 2443–2449.

Hutangura, P., Mathesius, U., Jones, M.G.K., and Rolfe, B.G. (1999). Auxin induction is a trigger for root gall formation caused by root-knot nematodes in white clover and is associated with the activation of the flavonoid pathway. Aust. J. Plant Physiol. **26,** 221–231.

Hutzler, P., Fischbach, R., Heller, W., Jungblut, T.P., Reuber, S., Schmitz, R., Veit, M., Weissenboeck, G., and Schnitzler, J.P. (1998). Tissue localisation of phenolic compounds in plants by confocal laser scanning microscopy. J. Exp. Bot. **49,** 953–965.

Jacobs, M., and Rubery, P.H. (1988). Naturally-occurring auxin transport regulators. Science **241,** 346–349.

Jung, W., Yu, O., Lau, S.M.C., O'Keefe, D.P., Odell, J., Fader, G., and McGonigle, B. (2000). Identification and expression of isoflavone synthase, the key enzyme for biosynthesis of isoflavones in legumes. Nat. Biotechnol. **18,** 208–212.

Kumagai, H., and Kouchi, H. (2003). Gene silencing by expression of hairpin RNA in *Lotus japonicus* roots and root nodules. Mol. Plant Microbe Interact. **16,** 663–668.

Limpens, E., Ramos, J., Franken, C., Raz, V., Compaan, B., Franssen, H., Bisseling, T., and Geurts, R. (2004). RNA interference in *Agrobacterium rhizogenes*-transformed roots of Arabidopsis and *Medicago truncatula*. J. Exp. Bot. **55,** 983–992.

Madsen, E.B., Madsen, L.H., Radutoiu, S., Olbryt, M., Rakwalska, M., Szczyglowski, K., Sato, S., Kaneko, T., Tabata, S., Sandal, N., and Stougaard, J. (2003). A receptor kinase gene of the LysM type is involved in legume perception of rhizobial signals. Nature **425,** 637–640.

Markham, K.R. (1982). Techniques of Flavonoid Identification. (London: Academic Press).

Markham, K.R. (1989). Flavones, flavonols and their glycosides. In Methods in Plant Biochemistry, P.M. Dey and J.B. Harbourne, eds (London: Academic Press), pp. 197–235.

Mathesius, U., Bayliss, C., Weinman, J.J., Schlaman, H.R.M., Spaink, H.P., Rolfe, B.G., McCully, M.E., and Djordjevic, M.A.

(1998b). Flavonoids synthesized in cortical cells during nodule initiation are early developmental markers in white clover. Mol. Plant Microbe Interact. **11,** 1223–1232.

Mathesius, U., Schlaman, H.R.M., Spaink, H.P., Sautter, C., Rolfe, B.G., and Djordjevic, M.A. (1998a). Auxin transport inhibition precedes root nodule formation in white clover roots and is regulated by flavonoids and derivatives of chitin oligosaccharides. Plant J. **14,** 23–34.

McKhann, H.I., Paiva, N.L., Dixon, R.A., and Hirsch, A.M. (1997). Chalcone synthase transcripts are detected in alfalfa root hairs following inoculation with wild-type *Rhizobium meliloti*. Mol. Plant Microbe Interact. **10,** 50–58.

Muday, G.K., and DeLong, A. (2001). Polar auxin transport: Controlling where and how much. Trends Plant Sci. **6,** 535–542.

Müller, A., Guan, C.H., Gälweiler, L., Tanzler, P., Huijser, P., Marchant, A., Parry, G., Bennett, M., Wisman, E., and Palme, K. (1998). AtPIN2 defines a locus of Arabidopsis for root gravitropism control. EMBO J. **17,** 6903–6911.

Murphy, A., Peer, W.A., and Taiz, L. (2000). Regulation of auxin transport by aminopeptidases and endogenous flavonoids. Planta **211,** 315–324.

Neu, R. (1956). Aromatische borsäuren als bathochrome reagentien für flavone. Z. Anal. Chem. **151,** 328–332.

Nishimura, R., Hayashi, M., Wu, G.J., Kouchi, H., Imaizumi-Anraku, H., Murakami, Y., Kawasaki, S., Akao, S., Ohmori, M., Nagasawa, M., Harada, K., and Kawaguchi, M. (2002). HAR1 mediates systemic regulation of symbiotic organ development. Nature **420,** 426–429.

Noh, B., Murphy, A.S., and Spalding, E.P. (2001). Multidrug resistance-like genes of Arabidopsis required for auxin transport and auxin-mediated development. Plant Cell **13,** 2441–2454.

Pacios-Bras, C., Schlaman, H.R.M., Boot, K., Admiraal, P., Langerak, J.M., Stougaard, J., and Spaink, H.P. (2003). Auxin distribution in *Lotus japonicus* during root nodule development. Plant Mol. Biol. **52,** 1169–1180.

Peer, W.A., Bandyopadhyay, A., Blakeslee, J.J., Makam, S.I., Chen, R.J., Masson, P.H., and Murphy, A.S. (2004). Variation in expression and protein localization of the PIN family of auxin efflux facilitator proteins in flavonoid mutants with altered auxin transport in *Arabidopsis thaliana*. Plant Cell **16,** 1898–1911.

Peer, W.A., Brown, D.E., Tague, B.W., Muday, G.K., Taiz, L., and Murphy, A.S. (2001). Flavonoid accumulation patterns of transparent testa mutants of Arabidopsis. Plant Physiol. **126,** 536–548.

Penmetsa, R.V., Frugoli, J.A., Smith, L.S., Long, S.R., and Cook, D.R. (2003). Dual genetic pathways controlling nodule number in *Medicago truncatula*. Plant Physiol. **131,** 998–1008.

Peters, N.K., Frost, J.W., and Long, S.R. (1986). The flavone, luteolin, induces expression of *Rhizobium meliloti* nodulation genes. Science **233,** 977–990.

Peters, N.K., and Long, S.R. (1988). Alfalfa root exudates and compounds which promote or inhibit induction of *Rhizobium meliloti* nodulation genes. Plant Physiol. **88,** 396–400.

Radutoiu, S., Madsen, L.H., Madsen, E.B., Felle, H.H., Umehara, Y., Gronlund, M., Sato, S., Nakamura, Y., Tabata, S., Sandal, N., and Stougaard, J. (2003). Plant recognition of symbiotic bacteria requires two LysM receptor-like kinases. Nature **425,** 585–592.

Rashotte, A.M., Poupart, J., Waddell, C.S., and Muday, G.K. (2003). Transport of the two natural auxins, indole-3-butyric acid and indole-3-acetic acid, in Arabidopsis. Plant Physiol. **133,** 761–772.

Recourt, K., van Tunen, A.J., Mur, L.A., van Brussel, A.A.N., Lugtenberg, B.J.J., and Kijne, J.W. (1992). Activation of flavonoid biosynthesis in roots of *Vicia sativa* subsp. *nigra* plants by inoculation with *Rhizobium leguminosarum* biovar *viciae*. Plant Mol. Biol. **19,** 411–420.

Redmond, J.W., Batley, M., Djordjevic, M.A., Innes, R.W., Kuempel,

P.L., and Rolfe, B.G. (1986). Flavones induce expression of nodulation genes in *Rhizobium*. Nature **323,** 632–635.

Reed, R.C., Brady, S.R., and Muday, G.K. (1998). Inhibition of auxin movement from the shoot into the root inhibits lateral root development in Arabidopsis. Plant Physiol. **118,** 1369–1378.

Rolfe, B.G., Gresshoff, P.M., and Shine, J. (1980). Rapid screening for symbiotic mutants of *Rhizobium* and white clover. Plant Sci. Lett. **19,** 277–284.

Ryder, T.B., Hedrick, S.A., Bell, J.N., Liang, X., Clouse, S.D., and Lamb, C.J. (1987). Organization and differential activation of a gene family encoding the plant defense enzyme chalcone synthase in *Phaseolus vulgaris*. Mol. Gen. Genet. **210,** 219–233.

Schnabel, E.L., and Frugoli, J.F. (2004). The PIN and LAX families of auxin transport genes in *Medicago truncatula*. Mol. Genet. Genomics **272,** 420–432.

Schwalm, K., Aloni, R., Langhans, M., Heller, W., Stich, S., and Ullrich, C.I. (2003). Flavonoid-related regulation of auxin accumulation in *Agrobacterium tumefaciens*-induced plant tumors. Planta **218,** 163–178.

Searle, I.R., Men, A.E., Laniya, T.S., Buzas, D.M., Iturbe-Ormaetxe, I., Carroll, B.J., and Gresshoff, P.M. (2003). Long-distance signaling in nodulation directed by a CLAVATA1-like receptor kinase. Science **299,** 109–112.

Sheahan, J.J., and Rechnitz, G.A. (1992). Flavonoid-specific staining of *Arabidopsis thaliana*. Biotechniques **13,** 880–883.

Shirley, B.W., Kubasek, W.L., Storz, G., Bruggemann, E., Koorneef, M., Ausubel, F.M., and Goodman, H.M. (1995). Analysis of *Arabidopsis* mutants deficient in flavonoid biosynthesis. Plant J. **8,** 659–671.

Smith, N.A., Singh, S.P., Wang, M.B., Stoutjesdijk, P.A., Green, A.G., and Waterhouse, P.M. (2000). Gene expression: Total silencing by intron-spliced hairpin RNAs. Nature **407,** 319–320.

Spaink, H.P. (1998). Flavonids as regulators of plants development. In Phytochemical Signals and Plant-Microbe Interactions, J.T. Romeo, K.R. Downum, and R. Verpoorte, eds (New York: Plenum Press), pp. 167–177.

Stafford, H.A. (1990). Flavonoid Metabolism. (Boca Raton, FL: CRC Press).

Stenlid, G. (1976). Effects of flavonoids on the polar transport of auxins. Physiol. Plant. **38,** 262–266.

Subramanian, S., Graham, M.Y., Yu, O., and Graham, T.L. (2005). RNA interference of soybean isoflavone synthase genes leads to silencing in tissues distal to the transformation site and to enhanced susceptibility to *Phytophthora sojae*. Plant Physiol. **137,** 1345–1353.

Swarup, R., Friml, J., Marchant, A., Ljung, K., Sandberg, G., Palme, K., and Bennett, M. (2001). Localization of the auxin permease AUX1 suggests two functionally distinct hormone transport pathways operate in the Arabidopsis root apex. Genes Dev. **15,** 2648–2653.

van Noorden, G.E., Ross, J.J., Reid, J.B., Rolfe, B.G., and Mathesius, U. (2006). Defective long distance auxin transport regulation in the *Medicago truncatula super numeric nodules* mutant. Plant Physiol. **140,** 1494–1506.

Vogt, T., Pollak, P., Tarlyn, N., and Taylor, L.P. (1994). Pollination or wound-induced kaempferol accumulation in *Petunia* stigmas enhances seed production. Plant Cell **6,** 11–23.

Wagner, H., Bladt, S., and Zgainski, E.M. (1984). Plant Drug Analysis. (Berlin: Springer).

Wesley, S.V., et al. (2001). Construct design for efficient, effective and high-throughput gene silencing in plants. Plant J. **27,** 581–590.

Wingender, R., Roehrig, H., Hoericke, C., Wing, D., and Schell, J. (1989). Differential regulation of soybean chalcone synthase genes in plant defence, symbiosis and upon environmental stimuli. Mol. Gen. Genet. **218,** 315–322.

Winkel-Shirley, B. (2001). Flavonoid biosynthesis. A colorful model for genetics, biochemistry, cell biology, and biotechnology. Plant Physiol. **126,** 485–493.

This information is current as of March 20, 2019

Supplemental Data	/content/suppl/2006/06/01/tpc.105.038232.DC1.html
References	This article cites 67 articles, 22 of which can be accessed free at: /content/18/7/1617.full.html#ref-list-1
Permissions	https://www.copyright.com/ccc/openurl.do?sid=pd_hw1532298X&issn=1532298X&WT.mc_id=pd_hw1532298X
eTOCs	Sign up for eTOCs at: http://www.plantcell.org/cgi/alerts/ctmain
CiteTrack Alerts	Sign up for CiteTrack Alerts at: http://www.plantcell.org/cgi/alerts/ctmain
Subscription Information	Subscription Information for *The Plant Cell* and *Plant Physiology* is available at: http://www.aspb.org/publications/subscriptions.cfm